Charge-changing cross sections for 1–70-keV H^+ and H^0 in collisions with calcium and strontium metal vapors

M. Mayo, J. A. Stone, and T. J. Morgan
Physics Department, Wesleyan University, Middletown, Connecticut 06457
(Received 3 February 1983)

Absolute electron-transfer cross sections have been measured for H^+ and H^0 in collisions with Ca and Sr metal vapor targets for energies between 1 and 70 keV. The measurements include cross sections for single- and double-electron capture by H^+ and single-electron capture and loss by H^0. The single-electron capture cross section for H^+ incident has been calculated using the binary-encounter approximation, and agrees with experiment to within a factor of 2 for energies between 2 and 70 keV. The electron-detachment cross section for H^- in collisions with Ca and Sr is determined from the present measured data and previously measured charge-state equilibrium fractions. The high- and low-energy structure in the cross sections for single- and double-electron capture by H^+ are discussed in terms of the importance of inner-shell capture at high energies and a molecular picture at low energies, and the cross sections are compared to those for Mg and Ba targets published in a previous paper. The cross section for single-electron capture by H^0 rises at low energies; that for electron detachment from H^- decreases at low energies in agreement with theoretical predictions of Olson and Liu. This situation is discussed as the mechanism responsible for large negative-ion equilibrium yields at low energies for alkaline-earth targets.

I. INTRODUCTION

In a recent paper[1] cross sections for single (σ_{10}) and double (σ_{1-1}) electron capture in collisions of protons with Mg and Ba atoms were reported. This work was initiated to study alkaline-earth–metal vapor targets which up to that time had received little experimental or theoretical attention. The ensuing time has seen publication of differential cross section measurements for H^- formation in $H^+ + Mg$ collisions[2] and two extensive measurements of the D^- equilibrium yields (F_∞^-) in Mg, Ca, Sr, and Ba alkaline-earth–metal vapor targets over the D^+ energy range 0.3 to 3.0 keV (Ref. 3) and 1.25 to 100 keV.[4] Theoretical work has included calculation of potential energy curves for positive, negative, and neutral states of MgH (Ref. 5) and CaH,[3] and for neutral states of CaH, SrH, and BaH.[6] The F_∞^- measurements, apart from a basic place in a program to study proton–alkaline-earth collisions, were motivated by their significance in applications where one needs an intense negative ion beam. An intense D^- beam accelerated to high energies and then neutralized provides an energetic neutral beam for injection into fusion plasmas to heat and fuel the plasma.[7] Producing intense D^- beams for use in tandem accelerators and for polarized D^- ion sources[8] is of considerable interest in nuclear physics experiments.

The D^- equilibrium yields for Ca and Sr targets are particularly significant; they exhibit interesting structure and are large for energies below 2 keV. Between 4 and 10 keV, F_∞^- exhibits a broad plateau and rises abruptly as the energy decreases below 4 keV. At 0.5 keV F_∞^- reaches a maximum value of 35% in Ca and 50% in Sr.[3] The maximum in F_∞^- for a Sr target is the largest D^- equilibrium yield measured to date, and that for Ca is comparable to the maximum of ~34% at 0.3 keV for a Cs target[8,9] which had been, until the Sr measurement, the largest D^- equilibrium yield measured.

The intent in the present work was to extend the original Mg and Ba measurements of σ_{10} and σ_{1-1} to Ca and Sr targets and thus complete a study of H^0 and H^- formations in single collisions of protons with alkaline-earth atoms. In addition, because of the large D^- equilibrium yields in Ca and Sr, we wished to expand the measurements to include some pertinent cross sections which, coupled with published theoretical work, might contribute to understanding the mechanisms responsible for the large F_∞^- maxima found.

With the double-electron-capture cross section typically two orders of magnitude smaller than that for single-electron capture in most targets, the second-order process $D^+ \rightarrow D^0 \rightarrow D^-$ is the simplest likely mechanism for thick target D^- production. Measurement of σ_{0-1} and σ_{01} is then pertinent to an understanding of this process and to the large F_∞^- maximum in Ca and Sr. Also governing the F_∞^- yield is the electron-detachment cross section σ_{-10}

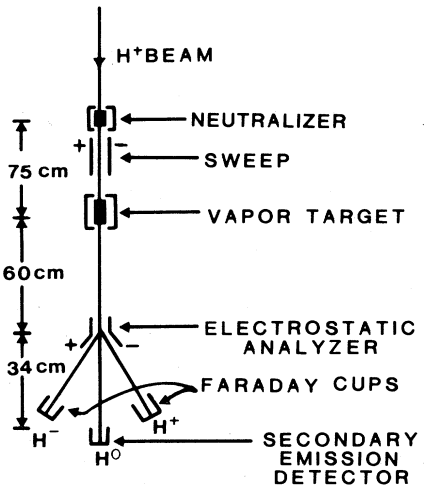

FIG. 1. Schematic diagram of the apparatus.

 ©1983 The American Physical Society

which, for a three—charge-state system, can be determined at low energies from F_∞^- and σ_{0-1}, and at high energies from F_∞^0 and F_∞^-, and the four cross sections σ_{10}, σ_{1-1}, σ_{01}, and σ_{0-1}.[10]

In this paper we report the measured cross sections σ_{10}, σ_{1-1}, σ_{01}, and σ_{0-1} for H^+ and H^0 incident on Ca over the energy range 1.0 to 30 keV and on Sr over the energy range 1.0 to 70 keV. The σ_{-10} cross section is determined from these measured cross sections and our previously measured equilibrium fractions for Ca and Sr targets over the respective energy ranges stated above. With this information and calculations for a Ca target,[3] the mechanisms for the structure and large yield in F_∞^- in Ca and Sr are discussed. Also, we have calculated σ_{10} using the binary encounter approximation.[11]

II. APPARATUS AND PROCEDURE

A. General description

A schematic diagram of the apparatus is shown in Fig. 1. With the exception of the equipment added for producing an incident H^0 beam, this apparatus has been described in detail in the report of our measurements of σ_{10} and σ_{1-1} for Mg and Ba targets.[1] Consequently, only a brief description of the overall apparatus and a detailed description of the preparation of the H^0 beam will be given in this section. In Ref. 1 the reader will find a detailed description of the preparation of the H^+ beam, the metal vapor target, the detection of the final charge components of the beam, and the cross-section analysis.

A proton beam was obtained from a radio-frequency ion source and accelerated to the desired energy between 1.0 and 70 keV. After momentum analysis and collimation, the H^+ beam was either passed through the metal vapor target for σ_{10} and σ_{1-1} measurements, or through the neutralizer cell described in Sec. II B below to prepare an H^0 beam which then passed through the scattering target for σ_{01} and σ_{0-1} measurements. An *in situ* analysis of the beam energy as a function of the accelerator energy and ion source parameters determined the beam energy spread to be ~ 80 eV; its mean energy is known to within ± 100 eV.

The metal vapor scattering target was a stainless-steel cylindrical chamber with a 1-mm-diam entrance and a 3-mm-diam exit aperture and an effective target length of 5.5 cm. Two resistive cartridge heaters embedded in the upper wall of the chamber heated the target, and two chromel-alumel thermocouples measured the target temperature. The target pressure was obtained by fitting the Clausius-Clayperon equation to vapor pressure versus temperature data of Hultgren *et al.*,[12] and cross sections were measured for Ca and Sr target thickness values (π) between 0.1 and 8×10^{13} cm^{-2}. Preceeding data acquisition, an adequate period of time was spent outgassing the oven at temperatures substantially higher than operating temperatures. During the outgassing and data acquisition periods the oven temperature was periodically cycled to ensure that oxide films did not inhibit evaporation of the pure metal.[13] The Ca metal was 99.9% pure and the Sr sample was guaranteed better than 99.5% pure.

The H^+ and H^- components were measured with Faraday cups and the H^0 component with a secondary electron emission detector; the scattered beam components were experimentally verified to be completely collected at the detectors. At each target thickness the secondary electron emission coefficient γ^+ for H^+ ions incident on the neutral atom detector was measured, and the relation $\gamma^0/\gamma^+ = 1.1$ was used to determine the coefficient γ^0 for incident H^0 atoms.[14] Background pressures in the target and detection apparatus were typically 2 to 5×10^{-7} Torr.

B. Neutralizer

For σ_{01} and σ_{0-1} measurements, a fraction of the H^+ beam from the accelerator undergoes neutralization after momentum analysis. The neutralizing apparatus consists of a retractable cell into which H_2 gas flows and an electric field which sweeps away the residual H^+ and H^- components in the beam. The neutralizing cell is a stainless-steel cylinder with removable apertures (2-mm-diam entrance and 3-mm-diam exit) on either end. A 113-mm Edwards diffstack oil diffusion pump provided typical neutralizer base pressures 1×10^{-7} Torr. Following the neutralizer housing a 720 V/cm electric field was set up between 9-cm-long plates.

The major concern in preparing the H^0 beam was confirming that 720 V/cm was a sufficient electric field to quench all H^0 ($2s$) metastable atoms, and to make negligible the effect of long-lived high-n excited states. In a 720 V/cm field, the metastable atoms have a lifetime less than 5×10^{-9} sec (Ref. 15) and thus decay to the ground state before reaching the target. Radiative decay during transit from neutralizer to target eliminates excited-state atoms with $n \leq 6$. The electric field E_n which ionizes the state n is given by[16]

$$E_n = (6.2\times 10^8 \text{ V/cm})/(n)^4 .$$

For a 720 V/cm field the states with $n \geq 30$ are eliminated. Assuming that states from $n=7$ to $n=30$ are left in the H^0 beam after passing through the sweep plates, one can estimate that this is about 1.3% of the neutral beam. This estimation uses the Il'in *et al.*[17] expression $\sigma_n/\sigma_0 = a_0/(n)^3$ where σ_n is the cross section for formation of Rydberg atoms in state n, and a_0 is measured by Il'in *et al.* to be of order unity for a thin H_2 target. We observed no change in measured cross sections when the sweep field was reduced from 720 V/cm to 480 V/cm. Morgan *et al.*[18] have investigated the effects of excited-atom impurities in an H^0 beam on σ_{01} and σ_{0-1} for Xe targets and found that altering the excited-atom population of the H^0 beam by a factor of 2 had no measurable effect on the cross sections.

III. DATA ACQUISITION AND ANALYSIS

The cross sections were measured by plotting the growth of a charge-state fraction of the total beam as a function of target thickness. At a fixed energy, a measurement of the total beam and the separate H^+, H^0, and H^- currents was made for 20 to 100 different values of target thickness π, taken while heating the target cell and cooling it down. The particle-beam currents were measured with electrometers. Data acquisition was controlled by a DEC 2060 time sharing system, interfaced to the experiment through an IBM 7046 device coupler. The com-

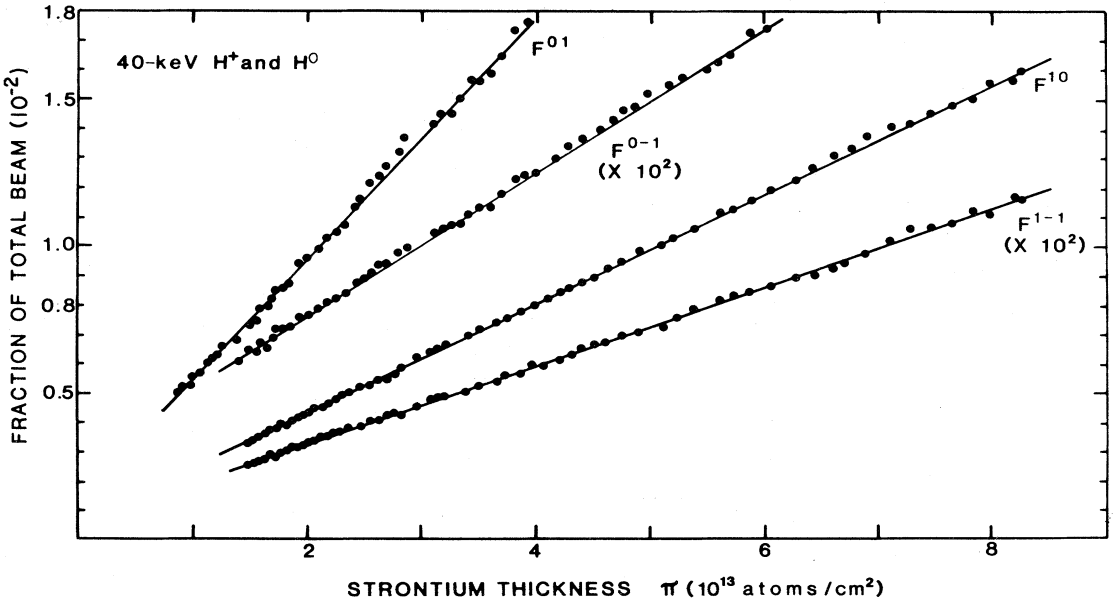

FIG. 2. Measured charge-state fractions as a function of Sr target thickness for a 40 keV incident beam. F^{01} and F^{0-1} are the H^+ and H^- fractions, respectively, for H^0 incident; F^{10} and F^{1-1} are the H^0 and H^- fractions, respectively, for H^+ incident.

puter controlled the operation of the deflector voltage which separated the final charge components of the beam as well as the data acquisition rate by monitoring the thermocouple voltage. This system routinely gathered data for several hours without operator intervention.

In a three—charge-state approximation, the fraction F^f of the total beam that goes from initial charge state i to final charge state f evolves as a function of the target thickness $\pi = nL$ (n=target number density; L=effective target length) according to

$$\frac{dF^f}{d\pi} = F^i\sigma_{if} + F^x\sigma_{xf} - F^f\sigma_{fl} \ . \tag{1}$$

In this equation, l denotes any charge-state loss mechanism and x the third charge state. The solution to Eq. (1), to second order in π, is given by[19,20]

$$F^f = \sigma_{if}\pi\left[1+\tfrac{1}{2}\pi\left[\frac{\sigma_{ix}\sigma_{xf}}{\sigma_{if}} - \sigma_{il} - \sigma_{fl}\right]\right] . \tag{2}$$

Under thin target single-collision conditions the solution to Eq. (1) reduces to the first-order term

$$F^f = \sigma_{if}\pi \ , \tag{3}$$

and cross sections may be obtained from the slope of F^f as a function of π. Figure 2 is typical of linear data taken during this experiment and the lines are a linear least-squares fit to the data.

If single-collision conditions cannot be satisfied in the experiment this simple procedure leads to errors in the cross-section measurement. In the present experiment at energies below about 5 keV, the negative fraction F^{-1} for protons incident had nonlinearities substantial enough that a linear region could not be experimentally verified even at the lowest π values feasible for a reliable H^- signal. Also, even if one has experimental verification of linearity between F^f and π, this may be too insensitive a test to verify single-collision conditions.[21,22] The magnitude of the second-order term in Eq. (2) was therefore checked for all of the fractions measured in the present experiment. As a result, the cross section σ_{1-1} required a correction calculated at each energy below 15 keV; the corrections ranged between 10% and 15%, and were due to the second-order process $H^+ \rightarrow H^0 \rightarrow H^-$.

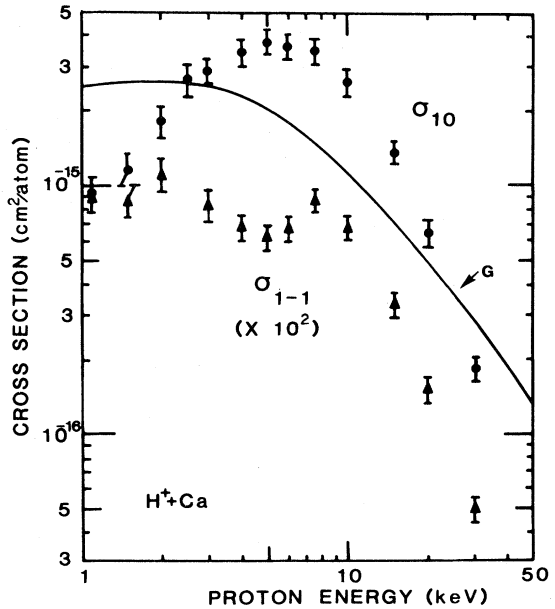

FIG. 3. Single- and double-electron-capture cross sections σ_{10} and σ_{1-1} for collisions of H^+ with Ca. σ_{10}: ●, present data using both H^+ and D^+ ions. σ_{1-1}: ▲, present data using both H^+ and D^+ ions. Curve G, present binary-encounter calculation of σ_{10}. The cross sections for D^+ ions have been plotted at $\frac{1}{2}$ the D^+ energy; no isotope effect was observed.

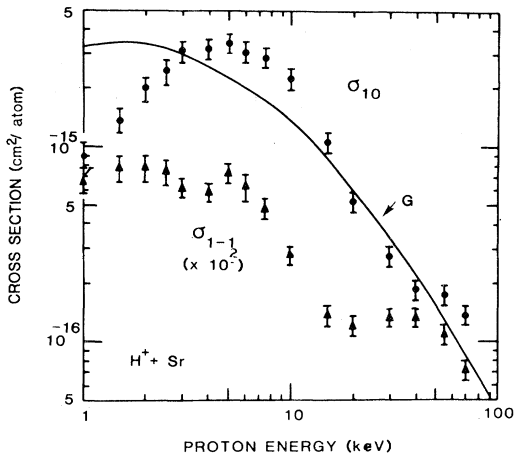

FIG. 4. Single- and double-electron-capture cross sections σ_{10} and σ_{1-1} for collisions of H^+ with Sr. σ_{10}: ●, present data using both H^+ and D^+ ions. σ_{1-1}: ▲, present data using both H^+ and D^+ ions. Curve G, present binary-encounter calculation of σ_{10}. The cross sections for D^+ ions have been plotted at one-half the D^+ energy; no isotope effect was observed.

Reproducibility of the data over a period of several months was ±10%. Relative uncertainties assigned to the data include reproducibility and, where appropriate, uncertainty introduced by a quadratic nonlinearity correction. The results also have a systematic uncertainty of ±20% based on knowledge of the vapor pressure.[12]

IV. RESULTS AND DISCUSSION

A. H^+ projectile

The present results for single- and double-electron capture for protons in collisions with Ca and Sr metal vapor targets are shown in Figs. 3 and 4, respectively. We have also computed a theoretical curve for the single-electron capture cross section (curve G) using the binary-encounter formalism.[11] In this model, a process $B^+ + A \rightarrow B + A^+$ has the classical binary-encounter cross section σ_c for single-electron capture in a single binary encounter given by[23]

$$\sigma_c = (\sigma_0 N_e)(U_B/U_A^3)[G(U_B/U_A; V_B/V_A)] , \quad (4)$$

where

$$G(U_B/U_A; V_B/V_A) = \frac{F(V_B/V_A)}{[1+(V_B/V_A)^2]^2 - (U_B/U_A)^2}$$

and

$$F(V_B/V_A) = (V_A/V_B)^2[V_B^2/(V_B^2+V_A^2)]^{3/2} .$$

In Eq. (4),

$$\sigma_0 = 1.312\times10^{-13}\ \text{eV}^2\text{cm}^2 ,$$

N_e is the number of equivalent electrons in the target subshell from which capture takes place, U_A and U_B are the binding energies of the electron before and after capture takes place. The velocity of the incident ion is V_B, the velocity V_A that of the electron in the target atom. Since the formalism is classical, we used the relation $V_A = (2U_A/m)^{1/2}$, where m is the electron mass, in carrying out the calculation.

The shortcomings of this formalism have been discussed extensively in the literature,[24–26] one obvious one being that the cross section is infinite [the denominator in Eq. (4) goes to zero] whenever $U_B > U_A$ and the projectile has energy

$$E = (M_B/m)(U_B - U_A) ,$$

where M_B is the projectile mass, and m is the electron mass. For all alkaline-earth atoms $U_B > U_A$ for capture from the outermost target shell into the hydrogen ground state, and expression (4) diverges for these capture processes. In this case the cross section was calculated via detailed balance[24] using the reverse reaction at equal ion velocity in Eq. (4). If E is the proton impact energy, then the cross section $\sigma_c(E)$ for a Ca target is equal to the cross section $\sigma_{DB}(E)$ for the reverse reaction with[24]

$$\sigma_{DB}(E) = \frac{\omega_f}{\omega_i}\sigma_c(\text{Ca}^+(^2S_{1/2}) + \text{H}(1s) \rightarrow \text{Ca}(^1S_0) + \text{H}^+; \tau E) , \quad (5)$$

where $\tau = m_{\text{Ca}}/m_{\text{H}^+}$, ω_f is the degeneracy of the $Ca^+ + H$ reactants, and ω_i is the degeneracy of the $Ca + H^+$ reactants, and σ_c is computed using Eq. (4) at incident Ca^+ energy τE.

The curves G in Figs. 3 and 4 are the sum of partial cross sections for capture into $n=1$ and $n=2$ hydrogen states and include contributions for capture from the three outermost target subshells.[19] Although binary-encounter calculations are not expected to be reliable below about 20 keV, the calculation of σ_{10} is seen to agree with the measurements within about a factor of 2 over the two decades in energy from 100 keV down to 2 keV. At the lowest and highest energies it generally overestimates σ_{10} by a factor of 2, and so, for a practical tool to easily estimate a

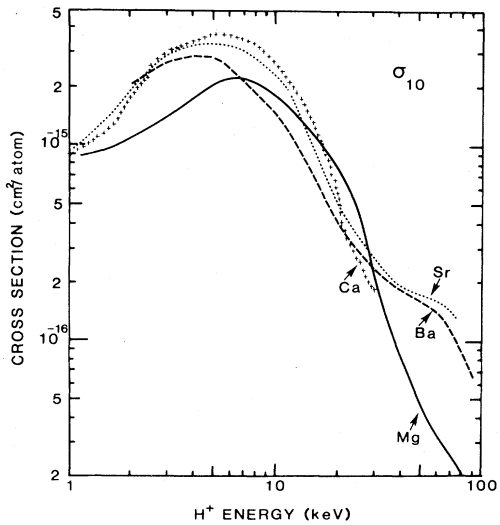

FIG. 5. Single-electron-capture cross section curves σ_{10} for collisions of H^+ with Mg (Ref. 1), Ba (Ref. 1), Sr, and Ca (present work) metal vapor targets.

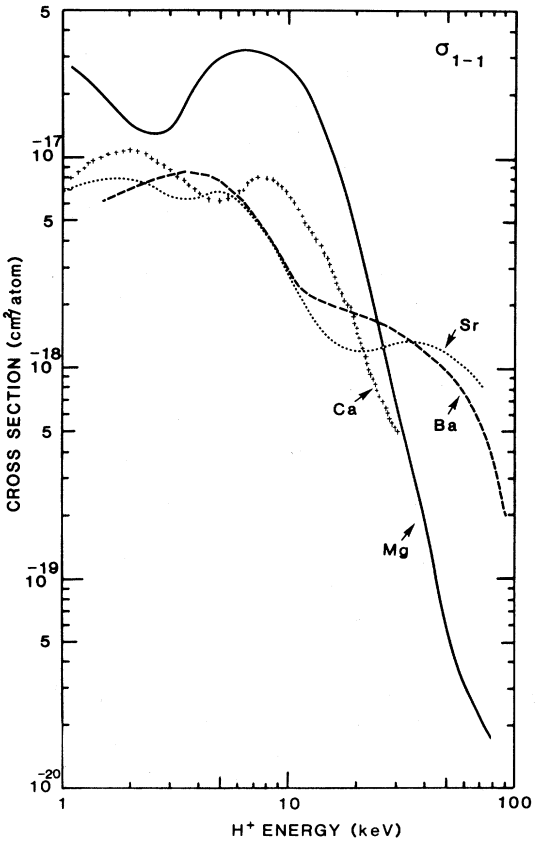

FIG. 6. Double-electron-capture cross section curves σ_{1-1} for collisions of H^+ with Mg (Ref. 1), Ba (Ref. 1), Sr, and Ca (present work) metal vapor targets.

single-electron-capture cross section, it appears no worse at low energies than at energies above about 50 keV.

Recently the binary-encounter formalism has been reexamined by Tan and Lee.[27] For a region of intermediate impact velocities the cross section given by Eq. (4) has contributions from both electron capture and impact ionization, each contributing with different cross sections.[25,27] Within the framework of the binary-encounter formalism, Tan and Lee determine an impact velocity region for which both electron capture and impact ionization occur and the size of the two cross sections over this region in an effort to eliminate contributions of impact ionization in their calculation of the electron-capture cross section. We have also calculated σ_{10} using these modifications[19] but the results are in very poor agreement with the data. The reason for this is not clear since, for an argon target, we have reproduced the results of Tan and Lee which are in reasonable agreement with measured data.[27]

A composite curve of this laboratory's measurements of σ_{10} and σ_{1-1} for alkaline-earth targets is given in Figs. 5 and 6, respectively. The cross sections show a generalized similarity in their behavior for Ca, Sr, and Ba targets when compared as a group to the cross sections for a Mg target. In the previous paper[1] for Mg and Ba targets it was pointed out that, although one might expect low-energy near-resonant behavior of σ_{10} for a Ba target compared to Mg, the data do not support this expectation. Similar statements are true for Ca and Sr. All three species (Ca, Sr, and Ba) have at least six single-electron-capture channels (with target excitation) lying below the initial state contrasted to only two for $H^+ + Mg$ collisions. Several of these single-electron-capture channels for Ca, Sr, and Ba lie within 1 eV of the initial state, leading one to argue (using energy balance) for a large maximum in σ_{10} for Ca, Sr, and Ba targets at incident ion energies substantially less than 1 keV. The maxima in σ_{10} for Ca, Sr, and Ba do not support this conclusion: they are only about 30% higher than the maximum in σ_{10} for Mg, and they occur at about 5 keV for the three targets. As suggested in Ref. 1, since double-electron capture is negligible, direct excitation of the target (without charge transfer) may be the source of the nonresonant behavior of σ_{10} in Ca, Sr, and Ba. In support of this suggestion, all three species have one or more direct target excitation channels less than 2 eV above the initial channel which could be energetically competitive with those single-electron-capture channels that are close to the initial channel, thus reducing the probability of single-electron capture via these close single-electron-capture states.

The structure of σ_{1-1} for Ca, Sr, and Ba targets is clearly very different than that for Mg (see Fig. 6). At low energy Ca, Sr, and Ba double-electron-capture cross sections are in general substantially smaller than σ_{1-1} for Mg: their maxima are roughly a factor of 4 smaller than the maximum value for Mg. None of the three σ_{1-1} cross sections for Ca, Sr, and Ba rise below 2 keV. In the previous paper[1] it was argued that σ_{1-1} for a Mg target rises as the energy decreases below 2 keV because there is a curve crossing of the incident and final states at a reasonable internuclear separation $R_x \sim 6.6a_0$, with a_0 the first Bohr radius. For a Ba target the curve crossing of the $H^+ + Ba$ incident state and the $H^- + Ba^{2+}$ final state occurs at a very large internuclear separation $R_x \sim 77a_0$. The location of the crossings was determined assuming a constant potential energy for the $H^+ + (Atom)$ channel and the

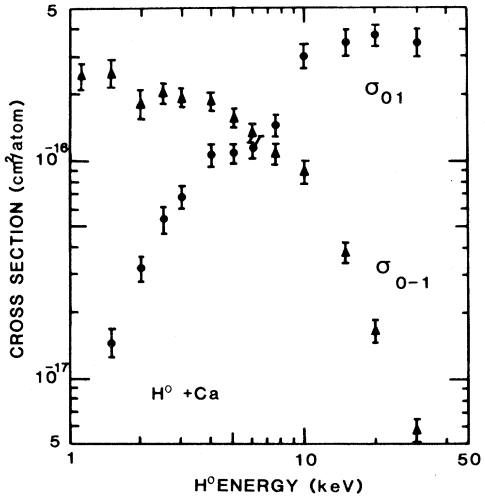

FIG. 7. Single-electron capture, σ_{0-1}, and loss, σ_{01}, cross sections for collisions of H^0 with Ca. σ_{0-1}: ▲, present data using both H^0 and D^0 atoms. σ_{01}: ●, present data using both H^0 and D^0 atoms. The cross sections for D^0 atoms have been plotted at one-half the D^0 energy; no isotope effect was observed.

Coulomb potential $(-2e^2/R)$ for the $H^- + (Atom)^{2+}$ channel, where e is the electron charge and R the internuclear separation. If the energy defect at infinite separation for the reaction $H^+ \rightarrow H^-$ is ΔE_∞, then

$$|-2e^2/R_x| = |\Delta E_\infty|$$

at the crossing point R_x. For Ca, $R_x \sim 15a_0$, and for Sr, $R_x \sim 23a_0$. As in the case for a Ba target, at such large separations the transition $H^+ \rightarrow H^-$ is far less likely than in the case of a Mg target.

At high energies both σ_{10} and σ_{1-1} exhibit structure which we attribute to electron capture from inner shells of the targets. For a Mg target Brinkman-Kramers calculations of Hiskes indicate that inner-shell capture becomes important at about 50 keV.[28] Although the present binary-encounter calculations for σ_{10} in Sr and Ca do not show explicit structure in the cross section at high energies, the calculation does predict capture from inner shells to dominate above about 50 keV.[19] This is consistent with the structure found in the experimentally determined σ_{10} cross section (see Fig. 5).

B. H^0 projectile

The present results for the single-electron capture (σ_{0-1}) and loss (σ_{01}) cross sections for H^0 in collisions with Ca are shown in Fig. 7 and those for Sr targets in Fig. 8. The σ_{01} and σ_{0-1} cross sections behave oppositely with energy. For energies above 8 keV, ionization of H^0, σ_{01}, becomes dominant. At 30 keV electron capture, σ_{0-1}, is two orders of magnitude smaller than ionization of H^0, and nearly three orders smaller at 60 keV. At low energies, ionization of H^0 (σ_{01}) falls by an order of magnitude between 10 and 2 keV while σ_{0-1} rises by about a factor of 3. Thus the D^- equilibrium yield rises (via the two-step process $H^+ \rightarrow H^0 \rightarrow H^-$) at low energies provided σ_{-10} is small.

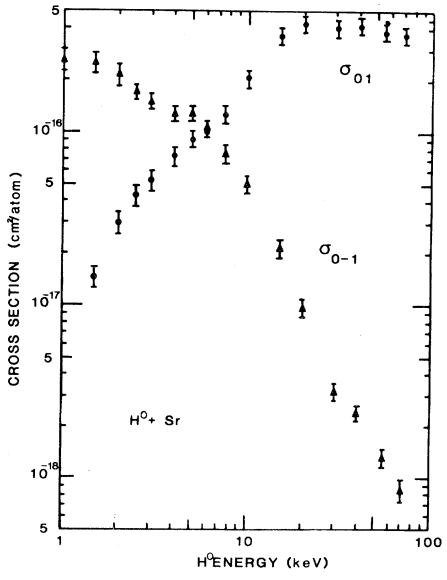

FIG. 8. Single-electron capture, σ_{0-1}, and loss, σ_{01}, cross sections for collisions of H^0 with Sr. σ_{0-1}: ▲, present data using both H^0 and D^0 atoms. σ_{01}: ●, present data using both H^0 and D^0 atoms. The cross sections for D^0 atoms have been plotted at one-half the D^0 energy; no isotope effect was observed.

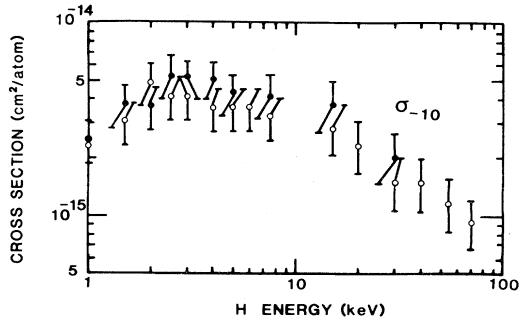

FIG. 9. Electron-detachment cross section σ_{-10} for H^- in collisions with Ca and Sr metal vapor targets. ●, Ca target; ○, Sr target.

We have calculated σ_{-10} for Ca and Sr targets over the energy range of the present data using the four cross sections σ_{10}, σ_{1-1}, σ_{01}, and σ_{0-1} reported in this paper and our previously measured[4] equilibrium fraction F_∞^- and unpublished measurements in this laboratory of F_∞^0. In the low-energy limit one can write[10]

$$\sigma_{-10} = \sigma_{0-1}[(1/F_\infty^-) - 1] . \tag{6}$$

Equation (6) requires $\sigma_{01}/\sigma_{10} \ll 1$, and two-electron processes (σ_{1-1} and σ_{-11}) must be negligible. These requirements are met quite well in Ca and Sr targets at 7.5 keV and below. At 15 keV and above a high-energy approximation of σ_{-10} was used[10]:

$$\sigma_{-10} = \frac{F_\infty^0}{F_\infty^-}\left[\frac{\sigma_{1-1}\sigma_{01}}{\sigma_{10}} + \sigma_{0-1}\right] . \tag{7}$$

Equation (7) requires that σ_{0-1}/σ_{01}, σ_{1-1}/σ_{10}, and $\sigma_{-11}/\sigma_{-10}$ all be much less than 1. These inequalities are met quite well in Ca and Sr above 30 keV and reasonably so between 15 and 30 keV. The values for F_∞^0 and F_∞^- at energies above 50 keV H^+ energy were extrapolated from our previous data.[4] The results of the calculation of σ_{-10} for Ca and Sr targets are shown in Fig. 9. For both targets σ_{-10} has a maximum around 2.5 keV and is falling for energies below 2 keV. This is in agreement with theoretical predications, based on *ab initio* molecular-interaction—energy calculations of the neutral and negative-ion CaH systems,[3] that both the charge-transfer and continuum electron detachment channels are small at low energies.

Correspondingly, when solved for F_∞^- at low energies, Eq. (6) becomes

$$F_\infty^- = [1 + (\sigma_{-10}/\sigma_{0-1})]^{-1} .$$

Our data show both that σ_{0-1} rises at low energy, and σ_{-10} decreases at low energy: this fortuitous situation results in a large negative-ion equilibrium fraction in heavy alkaline-earth—metal vapor targets.

ACKNOWLEDGMENTS

The authors would like to thank Claudia Clark for help in the initial stages of the experiment. This research was sponsored by the Office of Fusion Energy, U. S. Department of Energy and by Research Corporation.

[1]T. J. Morgan and F. J. Eriksen, Phys. Rev. A 19, 1448 (1979).
[2]I. Alvarez, C. Cisneros, and A. Russek, Phys. Rev. A 26, 77 (1982).
[3]R. H. McFarland, A. S. Schlachter, J. W. Stearns, B. Liu, and R. E. Olson, Phys. Rev. A 26, 775 (1982).
[4]T. J. Morgan, J. Stone, M. Mayo, and J. Kurose, Phys. Rev. A 20, 54 (1979).
[5]R. E. Olson and B. Liu, Phys. Rev. A 20, 1366 (1979).
[6]M. V. Ramanaiah and S. V. J. Lakshman, Physica 113C, 263 (1982).
[7]Proceedings of the Symposium on the Production and Neutralization of Negative Hydrogen Ions and Beams, Brookhaven National Laboratory, 1977, Report No. BNL-50727 (unpublished); H. P. Furth and D. L. Jassby, Phys. Rev. Lett. 32, 1176 (1974).
[8]A. S. Schlachter, K. R. Stalder, and J. W. Stearns, Phys. Rev. A 22, 2494 (1980).
[9]F. W. Meyer, J. Phys. B 13, 3823 (1980).
[10]H. Tawara and A. Russek, Rev. Mod. Phys. 45, 178 (1973).
[11]M. Gryzinski, Phys. Rev. 138, A336 (1965).
[12]R. R. Hultgren, P. D. Dlasi, D. T. Hawkins, M. Gleiser, K. K. Kelly, and D. D. Wagman, *Selected Values of Thermodynamic Properties of the Elements* (American Society for Metals, Cleveland, Ohio, 1973).
[13]J. C. Greenbank and B. B Argent, Trans. Faraday Soc. 61, 655 (1965).
[14]P. Pradel, F. Roussel, A. S. Schlachter, G. Spiess, and A. Valance, Phys. Rev. A 10, 797 (1974); J. Hill, J. Geddes, and H. B. Gilbody, J. Phys. B 12, 2875 (1979); J. E. Bayfield, Phys. Rev. 182, 115 (1969).
[15]Hans A. Bethe and Edwin E. Salpeter, *Quantum Mechanics of One- and Two-Electron Atoms* (Springer, Berlin, 1957), p. 287.
[16]F. Brouillard, in *Atomic and Molecular Processes in Controlled Thermonuclear Fusion,* edited by C. J. Joachain and D. E. Post (Plenum, New York, 1983).
[17]R. N. Il'in, I. Kikiani, V. A. Oparin, E. S. Solov'ev, and N. V. Federenko, Zh. Eksp. Teor Fiz. 47, 1235 (1964) [Sov. Phys.—JETP 20, 835 (1965)].
[18]T. J. Morgan, K. H. Berkner, W. G. Graham, R. V. Pyle, and J. W. Stearns, Phys. Rev. A 14, 664 (1976).
[19]M. Mayo, Ph.D. thesis, Wesleyan University, 1982 (unpublished).
[20]The negative sign in front of σ_{il} in Eq. (2) deserves comment. In many papers, e.g., Ref. 10 and Ref. 21, an expression for the negative fraction F^{-1} for protons incident gives the term $\sigma_{il}=(\sigma_{10}+\sigma_{1-1})$ a positive sign. This term is the loss of the primary beam which contributes in second order with a negative sign because there are fewer primary particles to make neutrals and negative ions.
[21]Ya. M. Fogel and R. V. Mitin, Zh. Eksp. Teor. Fiz. 30, 450 (1956) [Sov. Phys.—JETP 3, 334 (1956)]; Ya. M. Fogel, Usp. Fiz. Nauk 71, 243 (1960) [Sov. Phys.—Usp. 3, 390 (1960)].
[22]B. Hird and H. C. Suk, Phys. Rev A 14, 928 (1976).
[23]D. N. Tripathi and D. K. Rai, Phys. Rev. A 6, 1063 (1972).
[24]J. D. Garcia, E. Gerjuoy, and Jean E. Welker, Phys. Rev. 165, 72 (1968).
[25]L. Vriens, in *Case Studies in Atomic Collision Physics,* edited by E. W. McDaniel and M. R. C. McDowell (North-Holland, Amsterdam, 1969), Vol. 1.
[26]Robert A. Mapleton, *Theory of Charge Exchange* (Wiley, New York, 1972).
[27]C. K. Tan and A. R. Lee, J. Phys. B 14, 2399 (1981); 14, 2409 (1981).
[28]J. R. Hiskes, Lawrence Livermore Laboratory Report No. UCRL-50602, 1969 (unpublished).